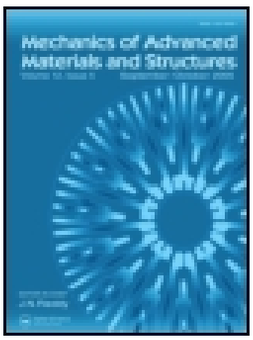

Mechanics of Advanced Materials and Structures

ISSN: 1537-6494 (Print) 1537-6532 (Online) Journal homepage: http://www.tandfonline.com/loi/umcm20

Experimental validation of a CFRP laminated/ fabric hybrid layout for retrofitting and repairing timber beams

Francisco J. Rescalvo, Elisabet Suarez, Chihab Abarkane, Ana Cruz-Valdivieso & Antolino Gallego

To cite this article: Francisco J. Rescalvo, Elisabet Suarez, Chihab Abarkane, Ana Cruz-Valdivieso & Antolino Gallego (2018): Experimental validation of a CFRP laminated/fabric hybrid layout for retrofitting and repairing timber beams, Mechanics of Advanced Materials and Structures, DOI: 10.1080/15376494.2018.1455940

To link to this article: https://doi.org/10.1080/15376494.2018.1455940

Published online: 10 Apr 2018.

MECHANICS OF ADVANCED MATERIALS AND STRUCTURES
2018, VOL. 0, NO. 0, 1–8
https://doi.org/10.1080/15376494.2018.1455940

Taylor & Francis
Taylor & Francis Group

ORIGINAL ARTICLE

Experimental validation of a CFRP laminated/fabric hybrid layout for retrofitting and repairing timber beams

Francisco J. Rescalvo[a], Elisabet Suarez[a], Chihab Abarkane[a], Ana Cruz-Valdivieso[b], and Antolino Gallego[a]

[a]Department of Applied Physics, Building Engineering School, University of Granada, Granada, Spain; [b]Department of Architectural Graphic Expression, Building Engineering School, University of Granada, Granada, Spain

ABSTRACT

This paper proposes a new hybrid layout to retrofit and repair timber beams by means of carbon composite material. It is based on the combination of a carbon laminate strip attached on the tension side, and a carbon fabric discontinuously wrapping the timber element. This layout has been experimentally validated by means of a study involving large-scale timber beams with many years in service. Results demonstrate not only that the bending load capacity of the broken beams can be totally recovered, but that it may even be increased by 70% with respect to the non-broken ones.

ARTICLE HISTORY
Received 13 March 2018
Accepted 13 March 2018

KEYWORDS
Timber; retrofitting; CFRP; repairing; bending load capacity

1. Introduction

Timber structures are used on all types of buildings and civil infrastructures around the world. The limited character of funding means that interventions must dedicate primarily to structures that require major repair to ensure safety and reliability over time. Yet it is becoming increasingly difficult to find large wooden elements for the replacement of structural members in buildings or infrastructures. In addition, their replacement is very costly and time-consuming. Retrofitting and repairing of structures or infrastructures should highly consider the use of innovative engineering techniques [1]–[5]. For this reason, strategies and technologies for on-site repair without eliminating existing structural members are of great interest and are highly valued commercially and technically. Wood members may be replaced or reinforced with concrete or metals [6]–[12]. However, some studies have explored the use of fiber-reinforced plastics (FRP) for the recovery and reinforcement of wooden structural members. Wood is commonly used in combination with other engineering materials in the transportation and construction sectors. Hybrid wood/carbon/glass structures can prove less costly to manufacture. Moreover, there are structural (tenacity and low density) and environmental benefits to be derived from the use of renewable materials such as wood [13].

The use of FRP for reinforcement of wood structures was firstly introduced in the sixties, when some authors [14]–[16] demonstrated that GFRP (fiberglass) installed wrapping the wood element in U shape produces a significant increasing of its ultimate strength, and an increasing of ductility (which is of vital importance for the structural safety), and makes the wood element able to endure greater deflections. Improvements of 50% and 20% in strength and stiffness, respectively, were obtained by some authors by means of the use of GFRP [17], [18].

Triantafillou and collaborators reported relevant results about the reinforcement with a carbon fiber reinforced polymer (CFRP) pultruded laminates placed on the bottom side of the timber [19], [20]: (1) failure pattern of the specimen changes from brittle to ductile and (2) an 1% of CFRP material of the cross-sectional area produces an increase in resistance of 60%; Fiorelli and Dias [21] indicated that, depending on the type (GFRP or CFRP) and amount of material (from 0.4% to 3%), stiffness increases from 15% to 60%. Valluzzi et al. [8] used CFRP sheets. The ultimate strength improved up to 100%. They also reported the great importance of the humidity conditions of the wood during the CFRP-wood adhesion process. Similar studies can be found in [22]–[24].

The authors [25] compared four reinforcement layouts, considering both tension and compression zones for location of the FRP. Improvements were about 17%–27% in stiffness, 40%–53% in flexural strength, and 36%–68% in shear strength. They also considered some layouts of reinforcement wrapping the lateral sides of the wood beam, demonstrating that this solution produces a substantial improvement of the ductility. Similar results were obtained by the authors of [20], [25], [26], who proposed the use of sheets of CFRP fabric U-shaped fully wrapping the bottom and lateral faces of the wood specimen.

In this context, this paper proposes an experimental validation of a here proposed hybrid layout for repairing and reinforcing timber beams using CFRP. It consists of the combination of a laminate strip attached on the tension side and a CFRP fabric discontinuously wrapping the timber element. This study involves large timber beams (4.5 m long) of *Pinus Sylvestris L.* having defects—knots, grain deviations, fissures, and wanes—extracted from the roof of a historical building.

CONTACT Elisabet Suarez elisabetsv@ugr.es Department of Applied Physics, Building Engineering School, University of Granada, Campus Fuentenueva, C/ Severo Ochoa SN, 18071 Granada, Spain.
Color versions of one or more of the figures in the article can be found online at www.tandfonline.com/umcm.

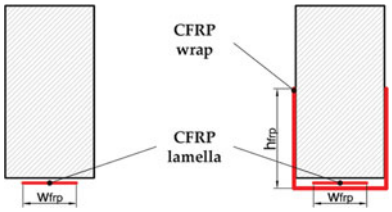

Figure 1. Reinforcement layouts. Left-hand side: LR. Right-hand side: BR.

2. Samples and mechanical tests description

The wood used (*P. Sylvestris* from southern Spain) for this study was extracted during the rehabilitation process of the Law Faculty of the University of Granada, which had been in service for 200–300 years. A total of six beams with a final cross section of $(147 \pm 11) \times (222 \pm 6)$ mm^2 and a length of 4500 ± 2.4 mm were selected. The mechanical properties of the wood were measured. In particular, the yielding compressive stress was 40 MPa with yielding strain of 3.6 mε. The maximum compressive stress was 48 MPa and the maximum strain was of 5.5 mε.

Two reinforcement layouts (longitudinal reinforcement and braided reinforcement, hereafter LR and BR, respectively; see Figures 1 and 2) were considered in this paper. LR layout has been widely used by other authors and is considered here only for comparison reasons. The other, BR, is a hybrid layout proposed in this paper, composed by a CFRP laminate wrapped by a discontinuously installed CFRP bidirectional fabric. The CFRP laminate in both reinforcement layouts was applied without covering the whole width of the beam, i.e. $w_{\mathrm{FRP}} = 100$ mm. The height of the CFRP fabric used in the BR was set at $h_{\mathrm{FRP}} = 150$ mm, as the minimum.

The CFRP and adhesives were supplied by DRIZORO® S.A.U. (hereafter, DRIZORO®). Specifically, the CFRP pultruded laminate was DRIZORO® COMPOSITE 1410 (width of 100 mm), while the CFRP fabric was DRIZORO® CARBOMESH 210 (bidirectional). The selected epoxy resin was MAXEPOX®-CS. To ensure a good CFRP-wood bond, pull-out and pull-off tests were carried out [27]. They allowed to properly selecting the used resin. The results of these tests are omitted for brevity reasons. The mechanical properties of CFRP pultruded laminates were 165,000 MPa and 2600 MPa for the elastic tensile modulus and ultimate tensile stress, respectively. For CFRP fabric, the ultimate tensile stress of the fiber and the elastic tensile modulus were of 4900 and 230,000 MPa, respectively. The application of reinforcement is described in detail in [28].

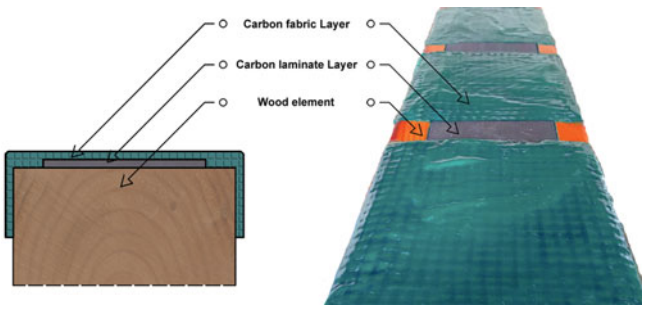

Figure 2. Graphic description of the BR layout. Image by authors.

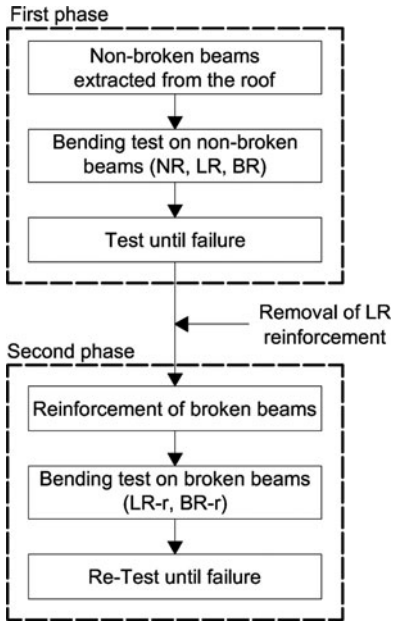

Figure 3. Phases of the experimental program.

Both reinforcement layouts, LR and BR, were tested under laboratory conditions in two experimental phases (Figure 3). During the first phase, beams directly extracted from the roof, previously subjected to a service load during 200 years, were tested. In the second phase, beams which were broken during the first phase in the laboratory were reinforced and tested again. The objective, in this second phase, was to evaluate the possibility of a total or partial recovery of a highly damaged element by using CFRP reinforcements.

During the first phase, the experimental program considered six timber beams: two beams were reinforced with LR layout, two beams with BR layout, and two non-reinforced (NR) ones used for comparison.

For the second phase, the NR and LR broken beams previously tested until failure were recovered and restored with the BR layout. These beams were tentatively called as BR-r. In order to make a proper comparison between non-broken and broken beams, the same area (%) of reinforcing material was used in all cases. Furthermore, for comparison, one broken beam was restored with an LR-r. Table 1 gives the specimen nomenclature.

Table 1. Bending tests program. The non-reinforced beams were named as NR, the longitudinal reinforced beams as LR, and the braided reinforced beams as BR. To designate the restored beams, the letter -r was used.

Phase	Reinforcement class	CFRP	Number of beams	Short name
1. Non-broken beams	NR	—	2	NR
	LR	Laminate	2	LR
	BR	Laminate + bidirectional wrap B	2	BR
2. Restored broken beams (r)	LR	Laminate	1	LR-r
	BR	Laminate + bidirectional wrap B	4	BR-r

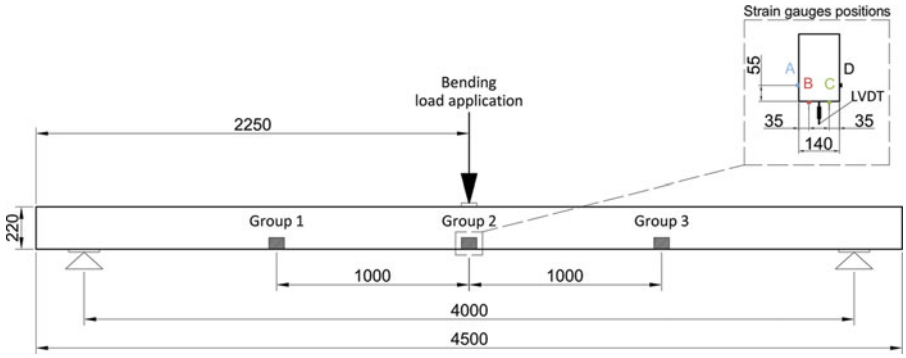

Figure 4. Experimental set-up (distances in mm).

Both non-broken and recovered broken beams were subjected to three-point bending tests, as Figure 4 shows. A monotonic loading was applied until final failure (displacement speed kept constant to 1.5 mm/min). Tests were performed on a machine from the company SERVOSIS S.L., CH4·ST·100 model. The span was set at 4000 mm between fixed supports, measuring the strains and deflections using strain gauges and linear variable differential transformers (LVDTs), respectively, with equipment from HBM, QUANTUMX MX 1615B model. For non-broken beams, three groups were established with four strain gauges and one LVDT for each group, as shown in Figure 4. For recovered broken beams, only strains and displacement at the mid-span (group 2) were measured.

3. Results

In order to compare both reinforcement layouts, a relative density, DC, was considered as [29]

$$\mathrm{DC} = \frac{\rho_m}{\rho_{\mathrm{beam}}} \tag{1}$$

where ρ_m is the density mean value and ρ_{beam} being the density of a particular beam. Therefore, the corrected module of rupture (MOR) is given by

$$\text{Corrected MOR} = \mathrm{DC} \times \mathrm{MOR}, \tag{2}$$

where MOR means the maximum bending capacity (module of rupture). The classification of types of failure was carried out according to the seven types considered in [30] (Figure 5).

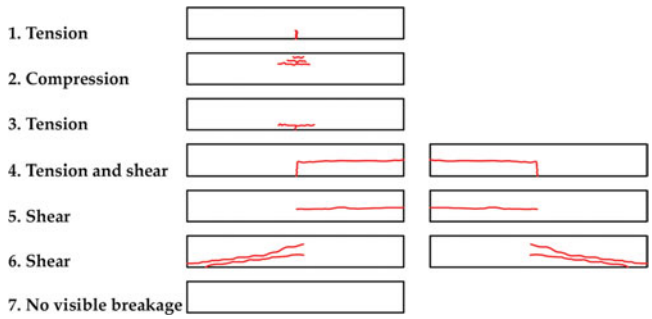

Figure 5. Types of failure [30].

3.1. *Phase 1. Non-broken beams*

Non-broken beams were divided into three groups, NR, LR, and BR. Figure 6 and Table 2 show the bending stress as a function of time, and the main mechanical properties for the control beams (NR).

For both NR beams, the mechanical behavior was elastic with a relevant dispersion between them and a brittle final failure. The average corrected MOR was of 16 MPa with an average modulus of elasticity (MOE) and maximum deflection of 7812 MPa and 35 mm, respectively. The final failure was caused by the knots located at the center of the beams, corresponding with the maximum tension zone (bottom of the beam), as seen in Figure 7, which depicts the typical failure pattern for this type of timber beam with defects.

Results from the strain analysis are shown in Figure 8, where higher strain values were reached by group 2 of strain gauges, placed at mid-span, corresponding to the maximum strain and deflection zone. Both NR beams had an elastic behavior until

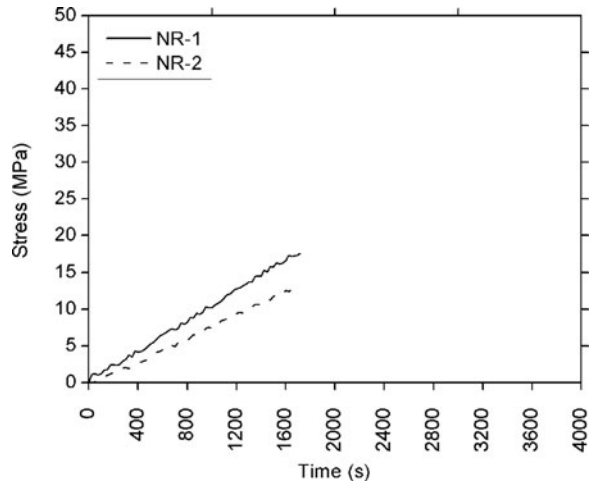

Figure 6. Bending stress vs. time for NR beams.

Table 2. Mechanical results for NR beams.

Name	MOR (MPa)	Density (kg/m^3)	Corrected MOR (MPa)	MOE (MPa)	Maximum deflection (mm)	Type of failure
NR-1	18	523	19	9239	35	3
NR-2	13	571	13	6384	35	4
Mean NR value	16	547	16	7812	35	—

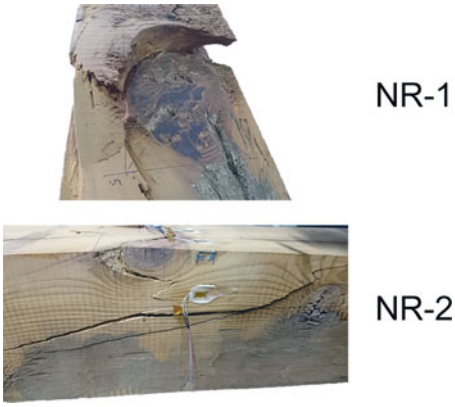

Figure 7. Failure patterns of NR beams. Top: NR-1. Bottom: NR-2. Image by authors.

Table 3. Mechanical results for longitudinal reinforced beams (LR).

Name	MOR (MPa)	Density (kg/m^3)	Corrected MOR (MPa)	MOE (MPa)	Maximum deflection (mm)	Type of failure
LR-1	34	562	33	13,483	63	4
LR-2	35	521	37	11,559	56	4
Mean LR value	35	541	35	12,521	60	—
Variation respect NR (%)	119	—	119	60	71	—

the final breakage, with no plastification in the compression zone. In addition, different stiffness values are shown according to the position of the strain gauge within the same group. Strain gauge 2B, for the NR-2 beam, measured irregular strains above a particular level of stress, mainly caused by the presence of knots.

Accordingly, Figure 9 and Table 3 show the results for the beams reinforced with LR layout. It can be observed that the

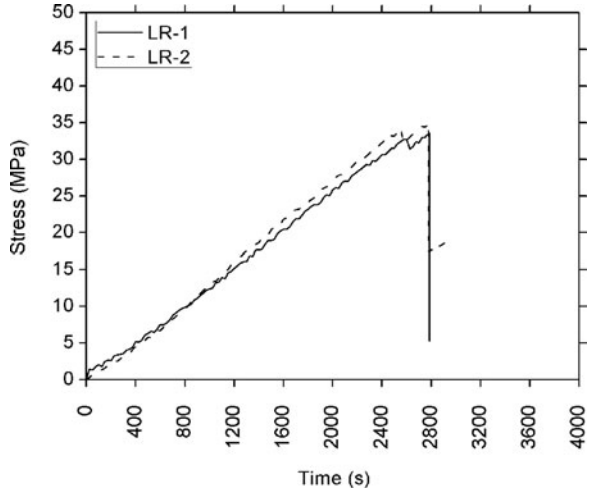

Figure 9. Bending stress vs. time for longitudinal reinforced beams (LR).

bending capacity was clearly improved for both specimens, a high stabilization of the mechanical properties and behavior being observed with respect to the NR beams. The corrected MOR increased a 119%, while the MOE and maximum deflection increased a 60% and 71%, respectively. As was predicted, these beams had a linear behavior until final breakage. Figure 10 shows some images corresponding to the two beams with a typical tension failure pattern owing to the important knots located at the tension zone, with a quick and subsequent delamination between timber and CFRP strip, due to the high stress values reached.

Figure 11 shows the strain analysis for the LR group. Remarkable are the higher values of maximum strains reached for group 2 and the increase in stiffness for all groups. Furthermore, a stabilization of the strain behavior was observed in knot-free zones for all the groups, while a slight plastification was observed in the compression zone.

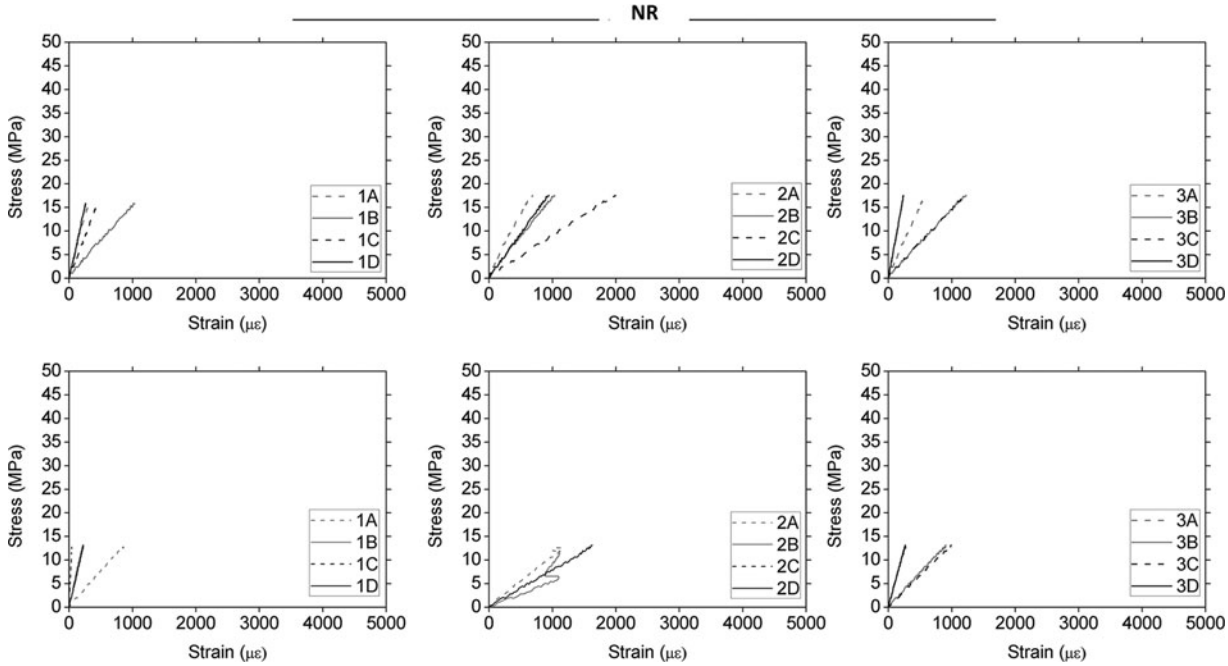

Figure 8. Stress vs. strain. Top: NR-1. Bottom: NR-2. Left-hand side: strain group 1. Center: strain group 2. Right-hand side: strain group 3.

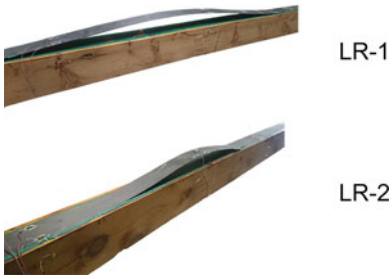

Figure 10. Failure patterns of the LR beams. Top: LR-1. Bottom: LR-2. Image by authors.

Finally, the bending stress versus time and the mechanical results for the braided reinforced beams are, respectively, shown in Figure 12 and Table 4.

A very significant improvement of all mechanical properties with regard to the NR and longitudinal reinforced beams is also clearly achieved. It is noteworthy that after reaching the maximum bending stress, the beams did not completely exhaust their strength capacity, remaining at 40% and 33% of the maximum value reached for BR-1 and BR-2 beams, respectively. After that point, the bending stress capacity increased again until a particular stress level, with no collapse of stress observed. In other words, a clear improvement in ductility is achieved by means of the braided reinforced layout as opposed to the NR and LR reinforced layouts. The corrected MOR improvement, MOE, and maximum deflection as opposed to NR beams were, respectively, 156%, 95%, and 71%, on average. Figure 13 shows the failure pattern for the two specimens, produced by a final slipping of the CFRP lamella followed by sudden delamination at the areas not covered by CFRP fabric.

Figure 14 displays the strain analysis up to the maximum bending stress. A clear improvement in stiffness, stability, and maximum strain is observed, respect to NR and LR beams. Plastification at the compression zone was observed at the zone of group 2 of the strain gauges. In other words, the mechanical properties of the wood were near their maximum limit.

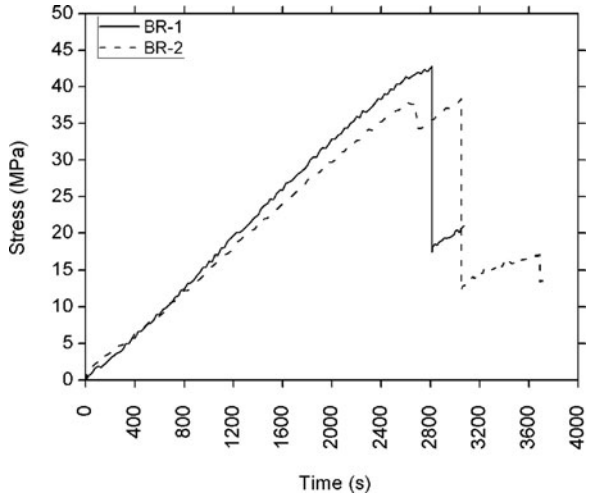

Figure 12. Bending stress vs. time for the braided reinforced beams (BR).

Table 4. Mechanical results for braided reinforced beams (BR).

Name	MOR (MPa)	Density (kg/m^3)	Corrected MOR (MPa)	MOE (MPa)	Maximum deflection (mm)	Type of failure
BR-1	43	469	50	16,858	60	4
BR-2	38	658	32	14,132	59	6
Mean BR value	41	564	41	15,495	60	—
Variation respect NR (%)	156	—	156	95	71	—

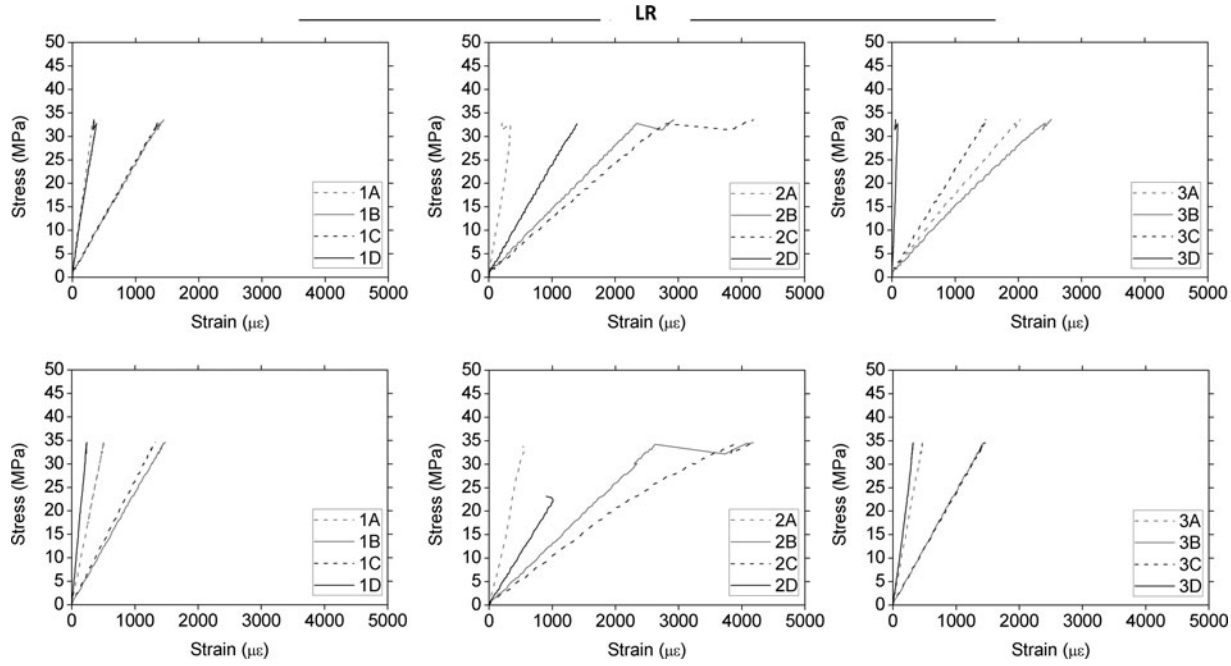

Figure 11. Stress vs. strain. Top: LR-1. Bottom: LR-2. Left-hand side: strain group 1. Center: strain group 2. Right-hand side: strain group 3.

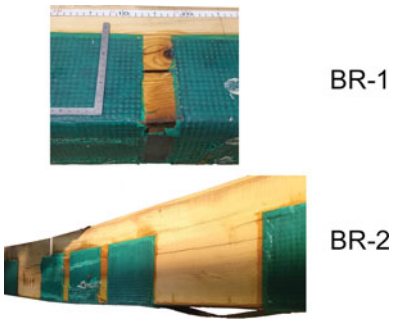

Figure 13. Failure patterns of the BR beam group. Top: BR-1. Bottom: BR-2. Image by authors.

3.2. *Recovered broken beams*

This section expands the results for the beams that were totally broken and then repaired, i.e. specimens LR-r and BR-r. Figure 15 and Table 5 show the results for LR-r beam.

As seen in Figure 15, and as predicted, a linear behavior was observed for this specimen. It is evident that a single lamella is not enough to fully recover the initial bending capacity of a beam. The corrected MOR was −31% of the non-broken NR elements, while the MOE and maximum deflection showed respective variations of 16% and −11%. Despite this decrease in the mechanical properties (except for MOE value), the beam reached acceptable values considering the high damage before repair.

In turn, results for the broken beams repaired with the BR layout are shown in Figure 16 and Table 6. This layout not only provided for full recovery of the bending capacity of the non-broken beam and a significant increase in ductility, but it led to an increase in the corrected MOR of 69%. This finding bears huge relevance when a broken beam needs to be repaired, since it is not necessary to disassemble a roof partially or completely when only some beams are damaged. Beam BR-r-3 does not show the ductile behavior observed in other cases because the test machine was close to the end of the stroke and the test had to be stopped for security. The mean MOE and maximum deflection improvements were of 35% and 109%, respectively. The remarkable increase of the maximum deflection (even improving upon the BR layout of the non-broken beams) was associated with the adaptation of the fabric placement for each beam.

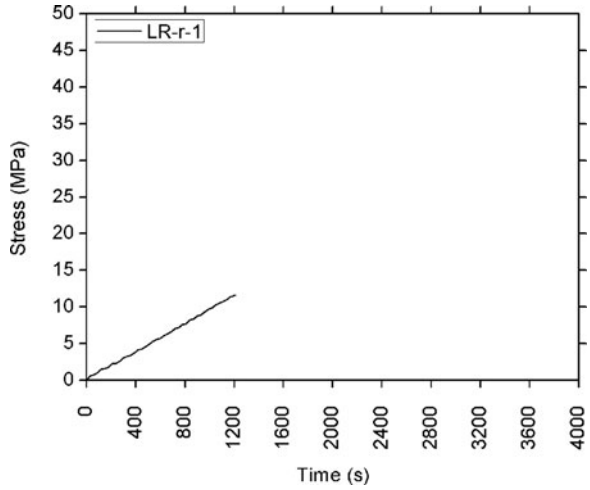

Figure 15. Bending stress vs. time for the repaired broken beams with the LR-r layout.

Table 5. Mechanical results for longitudinal reinforced beams (LR-r).

Name	MOR (MPa)	Density (kg/m^3)	Corrected MOR (MPa)	MOE (MPa)	Maximum deflection (mm)
LR-r-1	12	579	11	9067	31
Variation respect NR (%)	−25	—	−31	16	−11

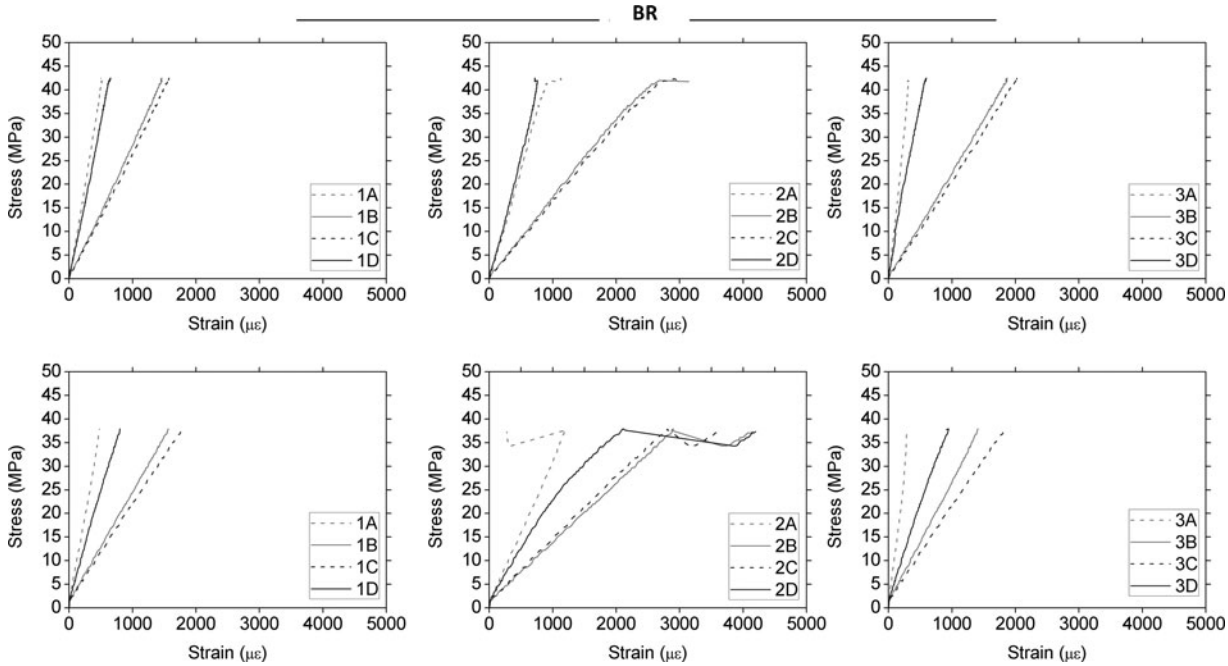

Figure 14. Stress vs. strain. Top: BR-1. Bottom: BR-2. Left-hand side: strain group 1. Center: strain group 2. Right: strain group 3.

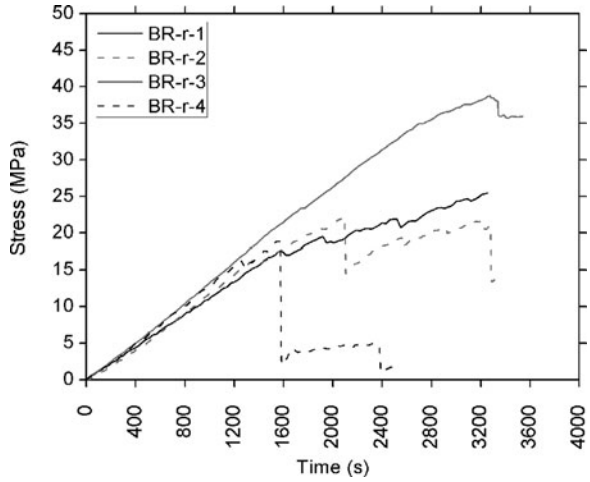

Figure 16. Bending stress vs. time for the repaired broken beams with the BR-r layout.

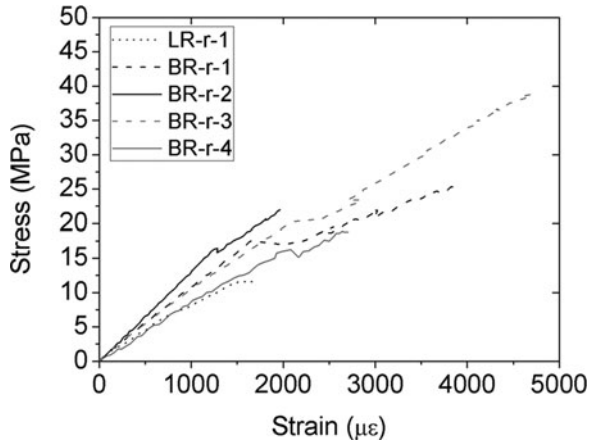

Figure 17. Stress vs. strain during bending tests for the strain gauge 2B.

Figure 17 displays the strain analysis for the strain gauge placed at the mid-span (maximum deflection) and at the tension side. In all cases, a linear behavior is observed until a particular level of stress, at which the beams appear to have a plastic behavior. Nevertheless, this change in slope was also associated with the reopening of existing cracks. Note that for all beams, the mean MOR value when the stress-strain slope changed was of 16 MPa, while the mean MOR for non-broken NR beams was of 16 MPa. This fact corroborates the total restoration of the mechanical properties by means of the BR reinforcement layout.

Table 6. Mechanical results for braided reinforced beams (BR-r).

Name	MOR (MPa)	Density (kg/m^3)	Corrected MOR (MPa)	MOE (MPa)	Maximum deflection (mm)
BR-r-1	25	562	25	10,825	75
BR-r-2	22	523	23	12,927	73
BR-r-3	39	521	41	9952	79
BR-r-4	19	571	18	8595	64
Mean BR-r value	26	544	27	10,575	73
Variation respect NR (%)	63	—	69	35	109

Figure 18. Damaged rafter before the repair process. Image by authors.

Figure 19. Rehabilitation process of the rafter. Left-hand side: placement of the CFRP lamella. Right-hand side: final state of the reinforced element. Image by authors.

4. On-site intervention

According to the laboratory results provided in previous sections, a real on-site application was carried out in a particular building. The repaired element was a rafter on the roof of the MADOC headquarter building. The rafter was seriously damaged on the tension side of the beam (Figure 18), for which reason the decision was made to apply the BR layout proposed in this paper.

Once the BR layout had been designed, it was necessary to recover in so far as possible the deflection of the beam with the help of mechanical jacks. After that, the reinforcement was applied following the same process as for laboratory specimen elaboration. Figure 19 shows images taken during the repairing process. Finally, after visual tracking, during one month, no application problems were detected.

5. Conclusions

An experimental analysis of a new hybrid layout using carbon composite as the reinforcement material to retrofit existent timber beams and to restore broken timber beams from buildings or infrastructures was carried out here. During the first phase of the experimental program, non-broken beams with more than 200 years in service were subjected to bending tests. Results for the NR beams showed an elastic mechanical behavior, without plastification, and a brittle final failure caused by knots located at the maximum tension center zone. The average corrected MOR was 16 MPa, the average MOE was 7812 MPa, and maximum deflection was 35 mm.

The non-broken beams with LR displayed a clearly improved mechanical behavior with respect to the NR beams: the corrected MOR was 119%, the MOE was 60%, and the maximum defection 71%. In this case, a slight plastification was exposed in the compression zone.

The proposed braided layout (BR), based on the combination of a carbon laminate strip attached on the tension side

and a carbon fabric wrapping the beam, provided a very substantial improvement of all mechanical properties and ductility, as opposed to the NR and LR beams. In this case, the timber reached the plastification range for its compressive stress. The improvement of the mechanical properties was: corrected MOR 156%, MOE 95%, and maximum deflection 71%.

During the second phase, four beams broken during the first phase were recovered and repaired with a BR-r layout and one with the LR-r layout. This paper concludes that although the LR layout was not enough to fully recover the initial bending capacity, the BR hybrid solution proposed provided remarkable improvements in corrected MOR, MOE, and maximum deflection, respectively, of 69%, 35%, and 109%, demonstrating its total capability for fully repairing broken wood elements. The solution was also verified during an on-site application on a highly damaged beam of the roof of a wooden structure in downtown Granada.

Acknowledgments

The authors gratefully acknowledge the important contribution of lab technicians David Jiménez and Ismael Romero.

Funding

This work was supported by the DÁVILA Restauración de Monumentos [contract no. 3546].

References

[1] A. Balsamo, M. Cerone, and A. Viskovic, "New wooden structures with composite material reinforcements for historical buildings: The case of the arena flooring in the Colosseum," Presented at the Proceedings of IABSE conference. Innovative wooden structures and bridges, August 29–31. Lahti, Finland, 2001.

[2] J. Jasieńko, *Glued and Engineering Joints in Repair, Conservation and Reinforcement of Historical Timber Structures*. Wrocław: Lower Silesia Educational Publishers (DWE), 2003.

[3] M. A. Parisi and M. Piazza, "Restoration and strengthening of timber structures: Principles, criteria, and examples," *Pract. Period. Struct. Des. Constr.*, vol. 12, no. 4, pp. 177–185, 2007.

[4] K. Schober and K. Rautenstrauch, "Post-strengthening of timber structures with CFRP's," *Mater. Struct.*, vol. 40, no. 1, pp. 27–35, 2007.

[5] T. P. Nowak, J. Jasieńko, and D. Czepiżak, "Experimental tests and numerical analysis of historic bent timber elements reinforced with CFRP strips," *Constr. Build. Mater.*, vol. 40, pp. 197–206, 2013. DOI: 10.1016/j.conbuildmat.2012.09.106.

[6] Y. J. Kim, M. Hossain, and K. A. Harries, "CFRP strengthening of timber beams recovered from a 32year old quonset: Element and system level tests," *Eng. Struct.*, vol. 57, pp. 213–221, 2013. DOI: 10.1016/j.engstruct.2013.09.028.

[7] P. Alam, M. P. Ansell, and D. Smedley, "Mechanical repair of timber beams fractured in flexure using bonded-in reinforcements," *Compos. Part B*, vol. 40, no. 2, pp. 95–106, 2009. DOI: 10.1016/j.compositesb.2008.11.010.

[8] M. R. Valluzzi, E. Garbin, and C. Modena, "Flexural strengthening of timber beams by traditional and innovative techniques," *J. Build. Appraisal*, vol. 3, no. 2, pp. 125–143, 2007. DOI: 10.1057/palgrave.jba.2950071.

[9] M. Corradi and A. Borri, "Fir and chestnut timber beams reinforced with GFRP pultruded elements," *Compos. Part B*, vol. 38, no. 2, pp. 172–181, 2007.

[10] A. Akbiyik, A. J. Lamanna, and W. M. Hale, "Feasibility investigation of the shear repair of timber stringers with horizontal splits," *Constr. Build. Mater.*, vol. 21, no. 5, pp. 991–1000, 2007.

[11] A. Borri, M. Corradi, and A. Grazini, "A method for flexural reinforcement of old wood beams with CFRP materials," *Compos. Part B*, vol. 36, no. 2, pp. 143–153, 2005. DOI: 10.1016/j.compositesb.2004.04.013.

[12] D. Radford, D. Van Goethem, R. Gutkowski, and M. Peterson, "Composite repair of timber structures," *Constr. Build. Mater.*, vol. 16, no. 7, pp. 417–425, 2002. DOI: 10.1016/S0950-0618(02)00044-2.

[13] M. P. Ansell, "Hybrid wood composites–integration of wood with other engineering materials," in *Wood Compos.*, vol. 54, pp. 411–426, 2015.

[14] F. Theakston, "A feasibility study for strengthening timber beams with fiberglass," *Can. Agric. Eng.*, vol. 7, no. 1, pp. 17–19, 1965.

[15] E. Biblis, "Analysis of wood-fiberglass composite beams within and beyond the elastic region," *Free Press J.*, vol. 15, pp. 81–88, 1965.

[16] R. Kellogg and F. Wangaard, "Influence of fiber strength on sheet properties of hardwood pulps," *TAPPI J.*, vol. 47, no. 6, pp. 361, 1964.

[17] R. Rowlands, R. Van Deweghe, T. L. Laufenberg, and G. Krueger, "Fiber-reinforced wood composites," *Wood Fiber Sci.*, vol. 18, no. 1, pp. 39–57, 1986.

[18] J. M. Moulin, G. Pluvinage, and P. Jodin, "FGRG: Fibreglass reinforced gluelam—A new composite," *Wood Sci. Technol.*, vol. 24, no. 3, pp. 289–294, 1990. DOI: 10.1007/BF01153561.

[19] T. C. Triantafillou and N. Deskovic, "Innovative prestressing with FRP sheets: mechanics of short-term behavior," *J. Eng. Mech.*, vol. 117, no. 7, pp. 1652–1672, 1991. DOI: 10.1061/(ASCE)0733-9399(1991)117:7(1652).

[20] T. C. Triantafillou, "Shear reinforcement of wood using FRP materials," *J. Mater. Civ. Eng.*, vol. 9, no. 2, pp. 65–69, 1997. DOI: 10.1061/(ASCE)0899-1561(1997)9:2(65).

[21] J. Fiorelli and A. A. Dias, "Analysis of the strength and stiffness of timber beams reinforced with carbon fiber and glass fiber," *Mater. Res.*, vol. 6, no. 2, pp. 193–202, 2003. DOI: 10.1590/S1516-14392003000200014.

[22] A. M. de Jesus, J. M. Pinto, and J. J. Morais, "Analysis of solid wood beams strengthened with CFRP laminates of distinct lengths," *Constr. Build. Mater.*, vol. 35, pp. 817–828, 2012. DOI: 10.1016/j.conbuildmat.2012.04.124.

[23] P. Neubauerová, "Timber beams strengthened by carbon–fiber reinforced lamellas," *Procedia Eng.*, vol. 40, pp. 292–297, 2012. DOI: 10.1016/j.proeng.2012.07.097.

[24] Y. J. Kim and K. A. Harries, "Modeling of timber beams strengthened with various CFRP composites," *Eng. Struct.*, vol. 32, no. 10, pp. 3225–3234, 2010. DOI: 10.1016/j.engstruct.2010.06.011.

[25] T. W. Buell and H. Saadatmanesh, "Strengthening timber bridge beams using carbon fiber," *J. Struct. Eng.*, vol. 131, no. 1, pp. 173–187, 2005. DOI: 10.1061/(ASCE)0733-9445(2005)131:1(173).

[26] A. Ajdukiewicz, J. Brol, A. Malczyk, and M. Wlaszczuk, "Rehabilitation of the highest wooden tower in Poland," *Struct. Eng. Int.*, vol. 10, no. 3, pp. 161–163, 2000. DOI: 10.2749/101686600780481572.

[27] F. J. Rescalvo, *Refuerzos De Fibra De Carbono Para Rehabilitación De Vigas De Madera. Modelos Analíticos, Ensayos Experimentales y Puesta En Obra*. Ph.D. dissertation, University of Granada, 2018.

[28] F. J. Rescalvo, I. Valverde-Palacios, E. Suarez, and A. Gallego, "Experimental comparison of different carbon fiber composites in reinforcement layouts for wooden beams of historical buildings," *Materials*, vol. 10, no. 10, pp. 1113, 2017. DOI: 10.3390/ma10101113.

[29] F. J. Rescalvo, I. Valverde-Palacios, E. Suarez, and A. Gallego, "Experimental and analytical analysis for bending load capacity of old timber beams with defects when reinforced with carbon fiber strips," *Compos. Struct.*, vol. 186, pp. 29–38, 2018. DOI: 10.1016/j.compstruct.2017.11.078.

[30] P. de la Rosa García, A. C. Escamilla, and M. N. G. García, "Bending reinforcement of timber beams with composite carbon fiber and basalt fiber materials," *Compos. Part B*, vol. 55, pp. 528–536, 2013. DOI: 10.1016/j.compositesb.2013.07.016.